Dalton Transactions

ROYAL SOCIETY OF CHEMISTRY

PAPER

View Article Online
View Journal | View Issue

Cite this: *Dalton Trans.*, 2025, **54**, 8612

Synthesis, structural characterization, and cytotoxic evaluation of monofunctional *cis*-[Pt(NH$_3$)$_2$(*N7*-guanosine/2′-deoxyguanosine)X] (X = Cl, Br, I) complexes with anticancer potential†

Asjad Ali, ‡ Gianluca Rovito,‡ Erika Stefàno, Federica De Castro, Giuseppe Ciccarella, Danilo Migoni, Elisa Panzarini, Antonella Muscella, Santo Marsigliante, Michele Benedetti * and Francesco Paolo Fanizzi

A series of new monofunctional platinum(II) complexes of the type *cis*-[Pt(NH$_3$)$_2$(*N7*-guanosine/2′-deoxyguanosine)X] (X = Cl, Br, I) were synthesized and characterized using NMR spectroscopy, mass spectrometry, and ICP-atomic emission spectroscopy. These complexes are designed to address the limitations of conventional bifunctional platinum-based drugs, such as cisplatin, which include issues with cytotoxicity and selectivity towards cancer cells. By incorporating guanosine or 2′-deoxyguanosine ligands and varying halido substituents, the study investigated how structural modifications influence the selectivity and cytotoxicity of the different analogues. To evaluate the anticancer potential of the newly synthesized platinum derivatives, various cancer cell lines were tested, including renal (Caki-1), uterine cervix (HeLa), breast (MCF-7), lymphoma (Raji), and mesothelioma (ZL-34). Additionally, selectivity against tumor cells was assessed by comparing their cytotoxic effects to those in the healthy, immortalized HK-2 cell line, a proximal tubular cell line derived from a normal human adult male kidney. Cytotoxicity analysis revealed that bromido-substituted Pt(II) complexes exhibited superior cytotoxicity across several cancer cell lines, particularly in HeLa and Raji cells, compared to their chlorido- and iodido-substituted counterparts. The iodido complexes exhibited higher efficacy against MCF-7 breast cancer cells, suggesting tumor-specific selectivity. Notably, these complexes demonstrated lower cytotoxicity in healthy cells compared to most of the tested cancer cell lines, as reflected by generally favorable selectivity indices (SI) relative to cisplatin.

Received 14th March 2025,
Accepted 24th April 2025

DOI: 10.1039/d5dt00616c

rsc.li/dalton

Introduction

Cancer is the leading cause of death worldwide, and the discovery of new, effective antitumor therapies is a primary objective of scientific research.[1] Platinum-based anticancer drugs play a pivotal role in medical oncology, particularly due to the widespread use of drugs like cisplatin, oxaliplatin, and carboplatin.[2–4] Approximately half of all patients undergoing anticancer chemotherapy are treated with a platinum-based drug.[3] These drugs primarily function by forming bifunctional DNA adducts, which inhibit DNA replication and transcription, ultimately leading to cell death. However, the development of drug resistance can result in the rapid repair of DNA damage and reduced drug accumulation.[3,5,6] Additionally, their non-specificity and lack of selectivity leads to undesirable side effects, highlighting the need to explore alternative platinum-based drugs with different mechanisms of action, cellular accumulation, and DNA-binding modes.[7–9]

Cationic monofunctional platinum(II) complexes, characterized by a single labile ligand, present a promising alternative to conventional platinum-based therapies. These complexes deviate from the traditional bifunctional mechanism and exhibit unique interactions with biomolecules, potentially reducing side effects and drug resistance.[8,10,11] Unlike cisplatin, each monofunctional platinum(II) complex can form only one covalent bond with DNA strands. Initially, monofunctional complexes similar to the inactive [Pt(dien)Cl]$^+$ and [Pt(NH$_3$)$_3$Cl]$^+$ complexes were also considered inactive against cancer cells, as it was believed that only *cis*-configured, square-planar, and neutral platinum(II) complexes could exhibit anticancer activity.[12–15] This assumption was challenged when cationic monofunctional *cis*-[Pt(NH$_3$)$_2$(Am)Cl]$^+$ complexes (where Am is an aromatic N-heterocyclic amine) were found to inhibit cancer cells *in vitro* and in mouse models of leukemia,

Department of Biological and Environmental Sciences and Technologies (DiSTeBA), University of Salento, Via Monteroni, I-73100 Lecce, Italy.
E-mail: michele.benedetti@unisalento.it

†Electronic supplementary information (ESI) available. See DOI: https://doi.org/10.1039/d5dt00616c

‡These authors contributed equally to this paper.

forming stable DNA adducts and demonstrating intercalative effects.[10,13,16,17] Recently, the discovery of the cationic monofunctional Pt(II) complex phenanthriplatin, *cis*-[Pt$(NH_3)_2$(phenanthridine)Cl]$^+$, has provided new insights into the development of platinum-based antitumor agents as alternatives to existing clinical drugs.[11,18,19] Due to the lipophilicity of its monodentate ligand, phenanthriplatin exhibits enhanced cellular uptake and greater cytotoxicity than cisplatin across various cancer cell lines.[3,5,18,20,21] Further research has shown that organic cation transporters (OCTs) play a role in the cellular uptake and activity of this type of cationic platinum(II) complexes.[22–24] Additionally, structure–activity relationship (SAR) analyses have demonstrated that steric hindrance of the adopted N-heterocyclic imine ligand is crucial. In fact, it can modulate the type of mono-adducts mainly formed with purines in DNA, and consequently the activity of RNA polymerase II.[18,25] The improved aqueous solubility, monofunctionality, and cationic nature of these platinum(II) complexes offer advantages over cisplatin analogs.[9]

Nucleotide analogues (NAs) are a class of compounds that include various pyrimidine and purine derivatives, commonly used as antiviral and anticancer agents.[26–30] NAs can function as antimetabolites, capable of interfering with nucleic acid synthesis or altering nucleoside metabolism.[31,32] Platinum-linked nucleosides may act as biomimetic substrates, facilitating selective cellular uptake and processing, potentially following pathways similar to those of other nucleoside analogue-based drugs.[27,33] This suggests that, once taken up by membrane transporters and phosphorylated, they may be recognized by nuclear or mitochondrial DNA polymerases and incorporated into newly synthesized DNA, leading to tumor cell death.[27] Therefore, we propose that the development of novel drug species based on NAs and other chemotherapeutics could enhance the therapeutic efficacy against various types of cancer.[34,35] In essence, these molecules could establish a new class of antitumor drugs by merging the properties of both nucleoside analogs and platinum-based drugs. The feasibility of this approach for anticancer applications of monofunctional *cis*-[Pt$(NH_3)_2$(Am)Cl]$^+$ (Am = heterocyclic amine) complexes has been evaluated in many studies using different complexes and *in vitro* and/or *in vivo* experimental approaches.[10,27,33,36–47]

In this study, we synthesized and evaluated the anticancer potential of six platinated nucleoside-based complexes. These complexes, of the type *cis*-[Pt$(NH_3)_2$(*N7*-guanosine)X] (X = Cl (**1**), Br (**2**), I (**3**)) and *cis*-[Pt$(NH_3)_2$(*N7*-2′-deoxyguanosine)X] (X = Cl (**d1**), Br (**d2**), I (**d3**)), represent a promising class of antimetabolites for cancer treatment. The choice of halide (Cl, Br, I) influences both the reactivity and stability of the complexes, as well as their interaction with biological targets.[48–50] By incorporating guanosine or 2′-deoxyguanosine ligands, which are intrinsically nontoxic and physiological, into the Pt(II) coordination sphere, we aim to enhance selectivity for cancer cells by mimicking natural nucleosides.[27] We synthesized new monofunctional platinum(II) complexes and tested their anticancer activity against various cancer cell lines. Additionally, we explored how structural modifications affect the selectivity and cytotoxicity of the different analogues tested in this study.

Results and discussion

Synthesis of *cis*-[Pt$(NH_3)_2$(*N7*-guanosine)X], X = Cl (1), Br (2), I (3), and *cis*-[Pt$(NH_3)_2$(*N7*-2′-deoxyguanosine)X], X = Cl (d1), Br (d2), I (d3), complexes

In this study, we present a new synthetic pathway for the production of a whole set of monofunctional, water-soluble platinum(II) complexes as possible promising candidates for anticancer applications. By varying the halido ligands in these monofunctional complexes, incorporating *N7*-guanosine (*N7*-Guo) and *N7*-2′-deoxyguanosine (*N7*-dGuo) ligands, we aimed to enhance their selectivity and efficacy in targeting cancer cells, already observed for the chlorido species.[10,36] As reported, besides the selection of other ligands, the halides choice is critical in determining the stability and biological activity of the resulting complexes.[51–53] Indeed, our findings indicate that substituting different halides is an effective strategy to modify the biological activities of these complexes while preserving their molecular structure.

The synthesis of *cis*-[Pt$(NH_3)_2$(Am)X]NO_3, where Am represents guanosine (*N7*-Guo) or 2′-deoxyguanosine (*N7*-dGuo) and X is either Cl or Br, follows a previously reported two-step method.[10,36,54] In the first step, *cis*-[Pt$(NH_3)_2X_2$] (X = Cl or Br) reacts with one equivalent of $AgNO_3$ in DMF, resulting in the formation of the monohalido species *cis*-[Pt$(NH_3)_2(NO_3)$X] and/or *cis*-[Pt$(NH_3)_2$(DMF)X](NO_3) (X = Cl or Br). These species contain oxygen-bound ligands, which act as superior leaving groups compared to chloride and bromide, thereby enhancing the Am coordination kinetics. In the subsequent step, these intermediates react with the guanosine (Guo) or 2′-deoxyguanosine (dGuo) ligands to yield the desired platinum complexes (**1–2** and **d1–d2**). The iodido complexes *cis*-[Pt$(NH_3)_2$(*N7*-Guo)I]$^+$ (**3**) and *cis*-[Pt$(NH_3)_2$(*N7*-dGuo)I]$^+$ (**d3**) were synthesized from the corresponding chlorido species (**1** or **d1**) by reaction with one equivalent of $AgNO_3$ in water and further addition of one equivalent of KI, after AgCl removal (Fig. 1).

The structural characterization of the resulting complexes was performed using a combination of techniques, including nuclear magnetic resonance (NMR) spectroscopy, mass spectrometry, and inductively coupled plasma atomic emission spectroscopy (ICP-AES).

NMR spectroscopy

The ^{1}H NMR spectra for all six platinum complexes (**1–3**, **d1–d3**) were collected and analyzed confirming the structure of the compounds. The spectra confirmed the nucleoside coordination in the metal complexes with chemical shifts variations according to the halido ligands (Cl, Br, I) attached to the platinum center. Key proton signals, including those for H8, NH_2 (of guanine), H1′, H2′, H2″, H3′, H4′, H5′, and H5″ (of the sugar moiety), and NH_3 (platinum-bound ammonia groups), were clearly assigned (Fig. 2 and S1†). The absence of the H2′ signal of compounds (**1–3**) and the H3′ signal of compounds (**d1–d3**) in ^{1}H NMR spectra is due to the overlapping with H_2O signal. Moreover, the variation in the total proton integration arises due to the presence of labile protons that undergo rapid

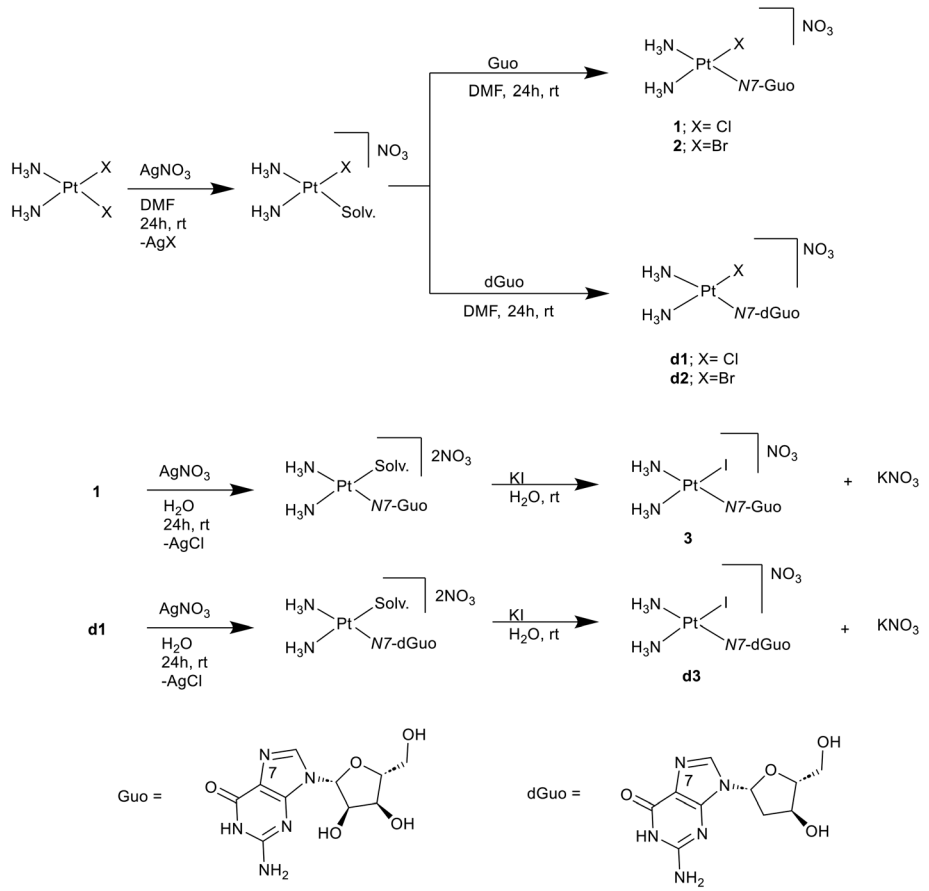

Fig. 1 Synthesis of platinum(II) nucleoside monoadducts: *cis*-$[Pt(NH_3)_2(N7\text{-Guo})X]^+$ (**1–3**) and *cis*-$[Pt(NH_3)_2(N7\text{-dGuo})X]^+$ (**d1–d3**) complexes, where X = Cl (**1**), Br (**2**), I (**3**).

exchange with the solvent. These exchangeable protons are often not observable (*e.g.*, –OH and –NH groups) or appear with reduced intensity (*e.g.*, $–NH_2$ and $–NH_3$ groups) under the conditions used. For each compound (**1–3**, **d1–d3**), the expected correlations between nucleoside protons coupled to each other within the complexes was confirmed using the $[^1H–^1H]$-COSY experiment, as reported in the literature.[55,56] The non-exchangeable protons of the sugar moiety resonate between 2.45 and 4.60 ppm. The NH_3 signals, appearing around 3.90–4.25 ppm, exhibit slight shifts across the spectra because of the different halido ligands bound to the platinum center. The observed chemical shifts variation for the NH_3 signals suggests that the halido ligands modulate the electronic structure of the platinum-nucleoside complex, affecting the chemical environment of the surrounding protons. This structural information is crucial for understanding how these different halido ligands influence the properties of the platinum complexes, potentially impacting their biological activity.

Comparison of the H8 proton chemical shifts of *N7*-Guo and *N7*-dGuo in platinum complexes also reveals distinct shifts depending on the halido ligands (Cl, Br, I). In all newly synthesized platinum complexes, the H8 proton resonates in the 8.36–8.46 ppm range. The H8 signals display a significant separation in chemical shifts, with the iodido complexes showing the highest downfield shifts and higher frequencies, followed by the bromido (**2** and **d2**), and then the chlorido complexes (**1** and **d1**). In contrast, all other peaks, including those of the sugar moiety and NH_3 protons, tend to shift slightly upfield (lower frequencies) by increasing the halogen size, with the effect most pronounced in the iodido complexes (**3** and **d3**). The observed trend can be attributed to the varying electronegativities and polarizabilities of the halido ligands, as well as the relative positions of the observed nuclei in relation to the occurring NMR magnetic shielding (Fig. 2 and S1†).[57]

To observe the direct coupling between the platinum center and nearby protons, such as those on the *N7*-Guo/*N7*-dGuo base and the ammonia ligands, 2D heteronuclear $[^1H,^{195}Pt]$ NMR spectra were acquired (Fig. 3 and S2†). The bidimensional spectra display three cross-peaks corresponding to NH_3 (*cis* to halido), NH_3 (*trans* to halido), and the H8 proton of the nucleobase moiety, all coupled with the central ^{195}Pt. Each platinum-nucleoside complex exhibits unique chemical shifts for the platinum center, influenced by the electronic properties of the halido ligands. Complexes with iodido ligands show the most shielded ^{195}Pt signals (**3** = $\delta(^{195}Pt)$ −2730 ppm, **d3** = $\delta(^{195}Pt)$ −2729 ppm), followed by bromido (**2** = $\delta(^{195}Pt)$ −2413 ppm, **d2** = $\delta(^{195}Pt)$ −2413 ppm) and chlorido (**1** = $\delta(^{195}Pt)$ −2282 ppm, **d1** = $\delta(^{195}Pt)$ −2282 ppm), indicating that

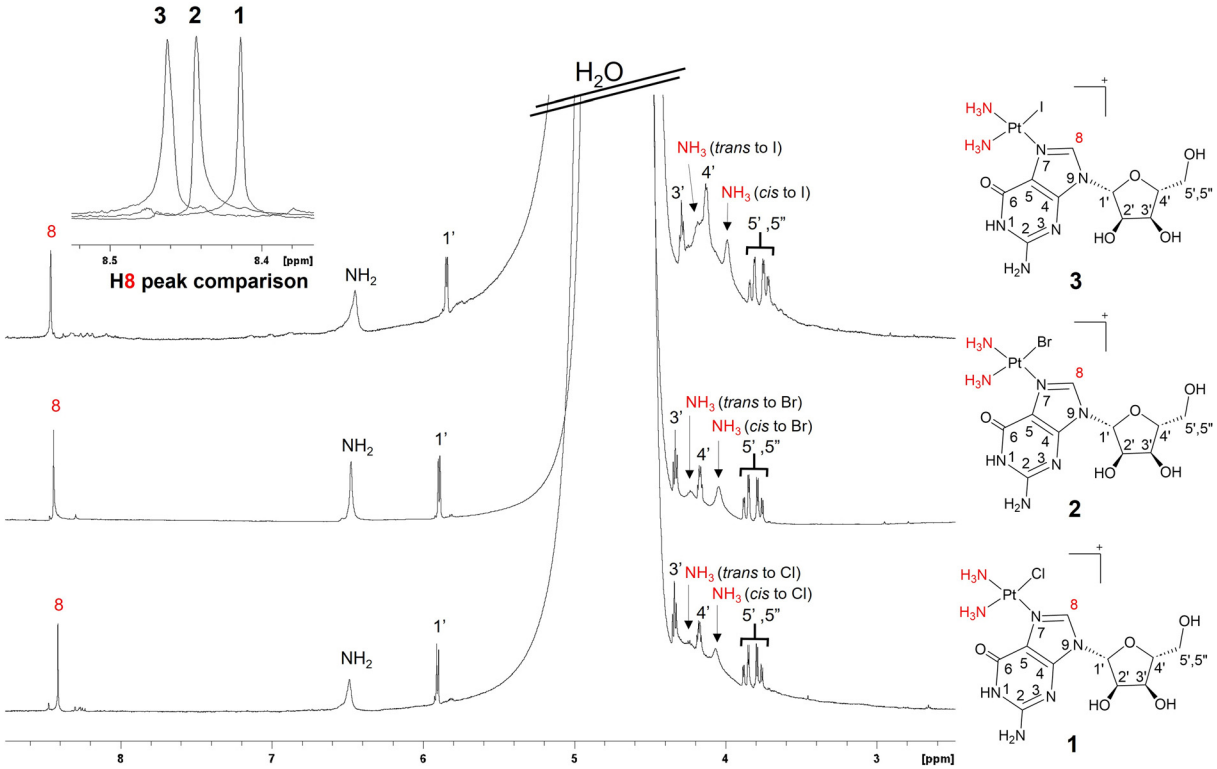

Fig. 2 ^{1}H NMR spectra of *cis*-[Pt(NH$_3$)$_2$(*N7*-Guo)X]$^+$ complexes, where X = Cl (**1**), Br (**2**), I (**3**), in H$_2$O/D$_2$O (90 : 10). The Pt-coupled NH$_3$ ligands and the H8 proton of *N7*-Guo are highlighted in red. The H2′ signal is masked by the broad signal of water.

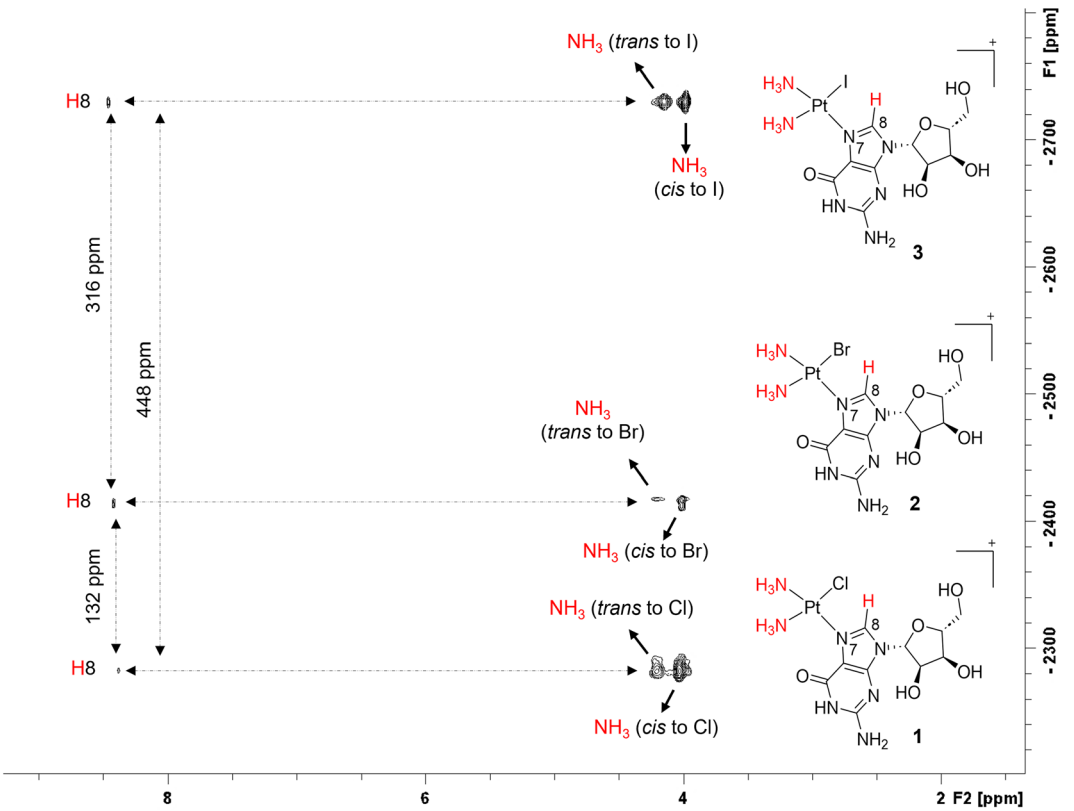

Fig. 3 [^{1}H,^{195}Pt]-HETCOR NMR spectra of the *cis*-[Pt(NH$_3$)$_2$(*N7*-Guo)X]$^+$ complexes, where X = Cl (**1**), Br (**2**), I (**3**), dissolved in H$_2$O/D$_2$O (90 : 10). The red labels indicate the groups, as shown in the structure above, that exhibit cross peaks in the 2D spectrum due to significant J_{H-Pt} couplings.

bulkier halido ligands lead to a more shielded platinum environment (Fig. 3). These findings align with previous studies[57–59] that indicate an inverse relationship between ^{195}Pt NMR chemical shifts and the cumulative ionic radii of halides.[57,60] The 2D NMR spectra also reveal different *cis* and *trans* NH_3 ligands. Where, coordinated NH_3's *trans* to halido ligand, show less intense cross peaks with ^{195}Pt, if compared to the corresponding signal for *cis* NH_3. This is because of the higher *trans* influence of the halido ligand, with respect to the *N7*-donor, reducing NMR coupling with ^{195}Pt, as previously reported.[10,36]

Mass spectrometry

The mass spectrometric analysis of the newly synthesized complexes was performed by dissolving them in water and using a HPLC-FT/MS Thermo Fischer Scientific Q-Exactive HPLC/HRMS instrument. The results were analyzed and compared with theoretical spectra[61] to assess the accuracy of the predicted mass-to-charge (m/z) ratios and isotopic distributions. The experimental spectra (Fig. S3†) revealed similar isotopic patterns for each complex, with peaks corresponding to the expected mass values, although slight deviations in m/z and relative abundances were observed. These deviations are expected in complexes containing platinum and halogens due to their inherently complex isotopic signatures. The experimental pattern, obtained directly from a high-resolution mass spectrometer, reflects the actual isotope ratios present in the sample, which may slightly differ from standard theoretical models assuming idealized natural abundances. For instance, platinum has multiple stable isotopes, and halogens contribute further complexity with their own isotope pairs. The observed discrepancies are likely due to slight variations in isotope ratios, instrument-specific response factors, or local isotope effects during ionization. The presence of the molecular ion peaks for the synthesized complexes at m/z $[M + H]^+$ 548.0776 (**1**), $[M + H]^+$ 532.0840 (**d1**), $[M + H]^+$ 592.0282 (**2**), $[M + H]^+$ 576.0326 (**d2**), $[M]^+$ 639.0171 (**3**), and $[M]^+$ 623.0216 (**d3**) is consistent with the proposed formulas of the corresponding

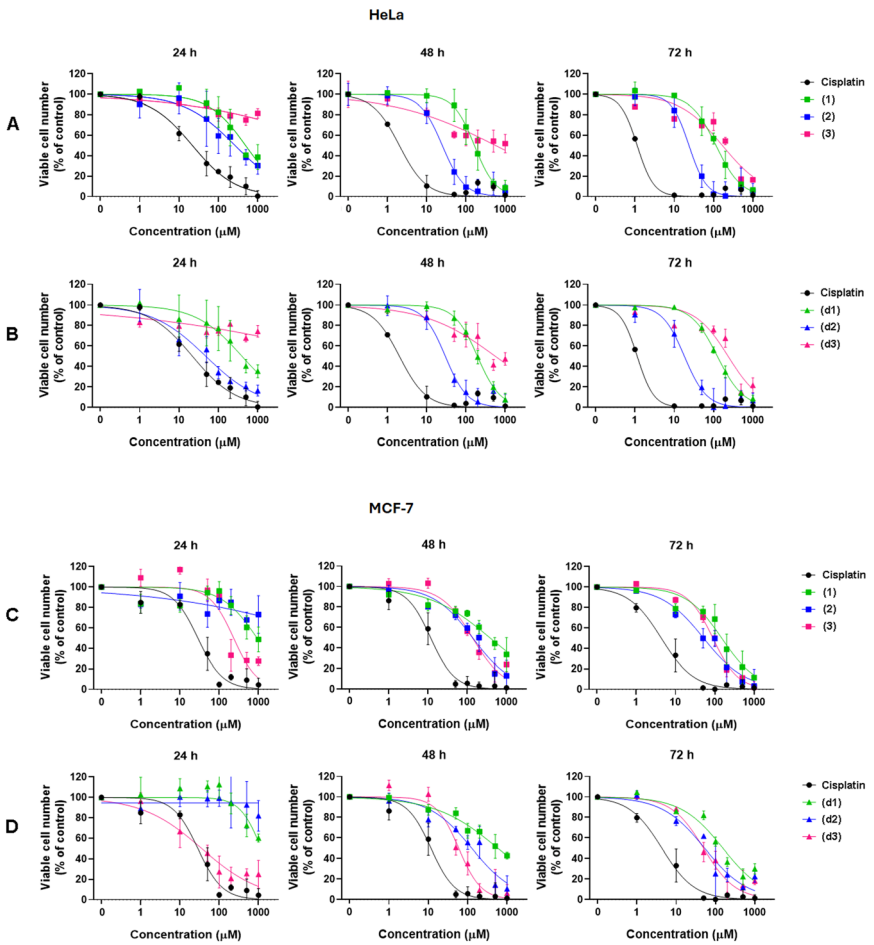

Fig. 4 Cytotoxic effects of cisplatin, *cis*-$[Pt(NH_3)_2(N7\text{-Guo})X]^+$ (panels A and C) and *cis*-$[Pt(NH_3)_2(N7\text{-dGuo})X]^+$ (panels B and D) complexes, where X = Cl (**1** and **d1**), Br (**2** and **d2**), I (**3** and **d3**), on cervical adenocarcinoma HeLa cells (panels A and B) and breast adenocarcinoma MCF-7 cells (panels C and D). These complexes were tested at concentrations ranging from 1 to 1000 μM over three incubation periods (24, 48 and 72 hours). Data is presented as the mean ± standard deviation from three independent experiments, each performed in eight replicates, and expressed as a percentage of the control.

complexes. In this context, "M" represents the corresponding platinum compound without NO_3. These results provide strong evidence for the successful synthesis of these target complexes.

Cytotoxicity studies

Fig. 4 and S10–S11† illustrate the cytotoxic effects of cisplatin and the platinum(II) nucleoside complexes *cis*-$[Pt(NH_3)_2(N7\text{-}Guo)X]^+$ (X = Cl, **1**; Br, **2**; I, **3**) and *cis*-$[Pt(NH_3)_2(N7\text{-}dGuo)X]^+$ (X = Cl, **d1**; Br, **d2**; I, **d3**). Cytotoxicity assays were performed using the SRB method for renal (Caki-1), uterine cervix (HeLa), breast (MCF-7), mesothelioma (ZL-34) and normal human kidney (HK-2) cells. However, for lymphoma (Raji) cells, which grow in suspension, the MTT assay was used, as it is more suitable for non-adherent cell cultures. Cytotoxic effects were evaluated over 24–72 hours of exposure. At 24 hours, cisplatin displayed greater cytotoxicity than most of the newly synthesized complexes in all tested cell lines, except for the Raji cells, where complex **2** was more cytotoxic. The highest cytotoxicity in every investigated cell line was exhibited by cisplatin for longer exposures (48 and 72 hours). Notably, at a concentration of 50 μM, cisplatin caused complete cell death in the pleural mesothelioma cell line (ZL-34) within 48 hours (Fig. S10†).

Among the new synthesized complexes, *cis*-$[Pt(NH_3)_2(N7\text{-}Guo)Br]^+$ (**2**) and *cis*-$[Pt(NH_3)_2(dGuo)Br]^+$ (**d2**) generally exhibited greater cytotoxicity than their chlorido (**1**, **d1**) and iodido (**3**, **d3**) counterparts, particularly in the HeLa cell line (see IC_{50} values in Table 1 and Fig. 4). Consistently, complexes **1**, **d1**, **3**, and **d3** were overall the least cytotoxic of the new synthesized series. In the case of the chlorido species (**1**, **d1**), their relatively higher propensity to halido ligand exchange with sulfur-containing biomolecules likely could hinder DNA targeting.[62] On the other hand, for the iodido complexes (**3**, **d3**), reduced aqueous stability and greater steric hindrance from the iodido ligand may reduce in some cases cytotoxic efficacy with respect to the other halido species. Nonetheless, it is noteworthy that after 24 hours of exposure, iodido complex **3** showed higher potency against MCF-7 cells than the other Guo-based complexes. This trend was also observed for the iodinated dGuo derivative **d3**, which proved to be the most cytotoxic compound against MCF-7 cells among all tested Guo and dGuo derivatives in the 24–72-hour timeframe (see IC_{50} values in Table 1).

Overall, the new Guo complexes were less toxic in renal (Caki-1) and mesothelioma (ZL-34) cancer cells, where the IC_{50} could often be determined only after 48–72 hours (Fig. S10 and S11;† Table 1). For instance, in Caki-1 cells, the IC_{50} for the iodido complexes **3** and **d3** exceeded 500 μM and could only be measured after 72 hours (Fig. S11;† Table 1). After 72 hours, ZL-34 cells remained relatively resistant to the chlorido derivatives (IC_{50} > 500 μM), whereas cell viability decreased

Table 1 Cytotoxic effects of cisplatin, *cis*-$[Pt(NH_3)_2(N7\text{-}Guo)X]^+$ (X = Cl, **1**; Br, **2**; I, **3**) and *cis*-$[Pt(NH_3)_2(N7\text{-}dGuo)X]^+$ complexes (X = Cl, **d1**; Br, **d2**; I, **d3**) on cervical adenocarcinoma (HeLa), sarcomatoid pleural mesothelioma (ZL-34), breast adenocarcinoma (MCF-7), lymphoma (Raji), renal carcinoma (Caki-1) and proximal tubule epithelial (HK-2) cells. Complexes were tested at concentrations ranging from 1 to 1000 μM over incubation periods of 24, 48 and 72 hours. Viable cells were determined using the SRB and the MTT assays. Data is presented as mean ± standard deviation from three independent experiments conducted in eight replicates, expressed as a percentage of the control. IC_{50} values are calculated and presented as mean ± standard deviation

IC_{50} (μM)							
	24 h	48 h	72 h		24 h	48 h	72 h
	HK-2				HeLa		
Cisplatin	52.74 ± 1.08	20.41 ± 1.14	15.85 ± 1.07	Cisplatin	21.92 ± 1.17	2.01 ± 1.17	1.14 ± 1.09
1	>1000	>1000	>1000	**1**	492.13 ± 1.17	164.24 ± 1.09	115.61 ± 1.09
2	>1000	661.36 ± 1.37	193.59 ± 1.15	**2**	265.99 ± 1.16	24.96 ± 1.15	23.73 ± 1.11
3	>1000	675.15 ± 1.16	724.91 ± 1.11	**3**	>1000	570.97 ± 1.53	168.36 ± 1.33
d1	>1000	>1000	>1000	**d1**	398.08 ± 1.31	195.44 ± 1.05	124.74 ± 1.04
d2	>1000	595.05 ± 1.20	175.09 ± 1.13	**d2**	47.91 ± 1.22	29.73 ± 1.05	18.09 ± 1.17
d3	>1000	>1000	>1000	**d3**	>1000	558.77 ± 1.33	234.33 ± 1.30
	MCF-7				**Raji B**		
Cisplatin	28.54 ± 1.17	11.65 ± 1.14	4.32 ± 1.12	Cisplatin	552.84 ± 1.31	29.51 ± 1.15	4.76 ± 1.14
1	921.45 ± 1.24	375.89 ± 1.18	148.93 ± 1.17	**1**	645.34 ± 1.42	136.16 ± 1.29	547.86 ± 1.18
2	>1000	137.05 ± 1.19	51.52 ± 1.22	**2**	210.49 ± 1.26	117.64 ± 1.36	86.04 ± 1.23
3	232.53 ± 1.33	135.80 ± 1.19	89.01 ± 1.10	**3**	>1000	>1000	>1000
d1	>1000	580.31 ± 1.16	154.38 ± 1.16	**d1**	>1000	501.14 ± 1.20	543.20 ± 1.39
d2	>1000	126.55 ± 1.26	52.99 ± 1.27	**d2**	615.56 ± 1.26	115.67 ± 1.34	124.37 ± 1.33
d3	35.69 ± 1.34	59.04 ± 1.18	49.62 ± 1.25	**d3**	>1000	756.39 ± 1.38	995.21 ± 1.48
	Caki-1				**ZL-34**		
Cisplatin	141.40 ± 1.21	24.20 ± 1.14	9.03 ± 1.15	Cisplatin	106.39 ± 1.20	14.84 ± 1.03	12.84 ± 1.09
1	>1000	714.41 ± 1.19	193.35 ± 1.11	**1**	>1000	>1000	>1000
2	>1000	395.02 ± 1.22	172.72 ± 1.22	**2**	>1000	470.75 ± 1.32	183.37 ± 1.18
3	>1000	>1000	557.90 ± 1.13	**3**	>1000	594.86 ± 1.11	543.47 ± 1.05
d1	>1000	482.71 ± 1.11	278.24 ± 1.15	**d1**	>1000	978.48 ± 1.48	588.28 ± 1.31
d2	>1000	428.87 ± 1.22	107.10 ± 1.24	**d2**	>1000	574.68 ± 1.28	189.09 ± 1.18
d3	>1000	>1000	767.93 ± 1.16	**d3**	>1000	485.75 ± 1.08	505.23 ± 1.05
					>1000	400–1000	200–400
					100–200	50–100	<50

upon exposure to the more cytotoxic bromido complexes **2** and **d2** (Fig. S10;† Table 2).

To further evaluate the antitumor potential of the *cis*-[Pt$(NH_3)_2$(*N7*-Guo)X]$^+$ (X = Cl, **1**; Br, **2**; I, **3**) and *cis*-[Pt$(NH_3)_2$(*N7*-dGuo)X]$^+$ (X = Cl, **d1**; Br, **d2**; I, **d3**) complexes, we calculated their selectivity index (SI), defined as the ratio of the IC_{50} in a normal immortalized proximal tubule epithelial cell line (HK-2) to that in each immortalized cancer cell line (HeLa, MCF-7, Raji, Caki-1, ZL-34) (Fig. 4, S10, S11;† Table 2). A value of SI greater than 1 indicates a higher specificity for cancer cells compared to healthy cells, while SI values above 4 classify the compound as highly selective (Table 2).[63] Several of the nucleoside-based complexes studied in this work exhibited SI values that exceeded those of cisplatin. To better identify the most selective complexes against each tumor cell line, we calculated an average SI across the 24-, 48-, and 72-hour intervals that we will indicate as SI_{AV} (Table 2). The principal factors affecting the SI_{AV} appear to be the type of cancer cell line and the identity of the halido ligand in the considered nucleoside derivatives. A secondary, yet still noteworthy, effect could be attributed to the presence of either Guo or dGuo.

Table 2 Selectivity indexes (SI) were calculated as the ratio of the IC_{50} values obtained for the normal immortalized proximal tubule epithelial cell line (HK-2) to those obtained for each cancer cell line (HeLa, MCF-7, Raji, Caki-1, or ZL-34). When one of the IC_{50} values exceeded 1000 μM, the SI could only be estimated. In these cases, SI values are reported exclusively if significant cytotoxicity was observed in the corresponding cancer cell line[a]

Selectivity index (SI)					
		24 h	48 h	72 h	SI_{AV}
HeLa (cervical adenocarcinoma)	Cisplatin	2.4	10.2	13.9	8.8
	1	>2.0[a]	>6.1[a]	>8.6[a]	>5.6
	2	>3.8[a]	26.5	8.2	>12.8
	3	—	1.2	4.3	2.75
	d1	>2.5[a]	>5.1[a]	>8.0[a]	>5.2
	d2	>20.9[a]	20.0	9.7	>16.9
	d3	—	>1.8[a]	>4.3[a]	>3.1
MCF-7 (breast cancer)	Cisplatin	1.8	1.8	3.7	2.4
	1	>1.1[a]	>2.7[a]	>6.7[a]	>3.5
	2	—	4.8	3.8	4.3
	3	>4.3[a]	5.0	8.1	>5.8
	d1	—	>1.7[a]	>6.5[a]	>4.1
	d2	—	4.7	3.3	4
	d3	>28.0[a]	>16.9[a]	>20.2[a]	>21.7
Raji (lymphoma)	Cisplatin	0.1	0.7	3.3	1.4
	1	>1.5[a]	>7.3[a]	>1.8[a]	>3.5
	2	>4.8[a]	5.6	2.3	>4.2
	3	—	<0.7[a]	<0.7[a]	<0.7
	d1	—	>2.0[a]	>1.8[a]	>1.9
	d2	>1.6[a]	5.1	1.4	>2.7
	d3	—	>1.3[a]	>1.0[a]	>1.2
Caki-1 (renal cancer)	Cisplatin	0.4	0.8	1.8	1
	1	—	>1.4[a]	>5.2[a]	>3.3
	2	—	1.7	1.1	1.4
	3	—	<0.7[a]	1.3	<1
	d1	—	>2.1[a]	>3.6[a]	>2.9
	d2	—	1.4	1.6	1.5
	d3	—	—	>1.3[a]	>1.3
ZL-34 (sarcomatoid pleural mesotelioma)	Cisplatin	0.5	1.4	1.2	1
	1	—	—	—	—
	2	—	1.4	1.1	1.3
	3	—	1.1	1.3	1.2
	d1	—	>1.0[a]	>1.7[a]	>1.4
	d2	—	1.0	0.9	1
	d3	—	>2.1[a]	>2.0[a]	>2.1

[a] IC_{50}(HK-2) or IC_{50}(tumor cell line) not measurable, since higher of maximum tested concentration (1000 μM). In this case, the not measurable IC_{50} value is assumed equal to 1000 μM for the estimation of the possible indicated minimum or maximum SI value.

In HeLa cancer cells, the bromo complex **d2** yielded the highest SI_{AV}, surpassing also its structural analog **2** (Table 2). Both complexes were more selective than cisplatin. The order of decreasing SI_{AV} for HeLa cells was **d2** > **2** > cisplatin > **1** > **d1** > **d3** > **3**. Interestingly, **d2** was also the most cytotoxic complex in HeLa cells among the tested nucleobase derivatives, followed by **2**. For this reason, both complexes **d2**, **2** appear promising antitumor drugs for HeLa cells related tumors.

In contrast, the iodido derivative **d3** (dGuo), followed by the iodido derivative **3** (Guo) showed higher selectivity for MCF-7 cells where cisplatin appeared the least selective. The order of decreasing selectivity for MCF-7 cells was **d3** ≫ **3** > **2** > **d1** > **d2** > **1** > cisplatin. Notably, **d3** was also the most cytotoxic complex for the cisplatin resistant MCF-7 tumor cells among tested nucleobase derivatives, followed by **3**. For this reason, both complexes seem promising antitumor drugs for tumor types related to MCF-7 cells.

In the Raji cells the bromido derivative **2** was the most selective, followed by the chlorido complex **1**, both showing higher selectivity than cisplatin (Table 2). The descending order of selectivity for Raji cells was **2** > **1** > **d2** > **d1** > cisplatin > **d3** > **3**. Complex **2** was also the most cytotoxic in Raji cells among the tested nucleobase derivatives, followed by **d2** and **1**. For this reason, both complexes could be considered promising antitumor drugs for tumor types related to Raji cells.

In Caki-1 the chlorido complexes **1** and **d1** were most selective, both exceeding cisplatin (Table 2). The descending order of SI_{AV} for Caki-1 was **1** > **d1** > **d2** > **2** > **d3** > cisplatin > **3**. Meanwhile, the significant cytotoxicity of **1** and **d2** for Caki-1 cells indicates that both complexes could be considered promising antitumor drugs for tumor types related to Caki-1 cells.

Lastly, in ZL-34 the iodido derivative **d3** exhibited the highest SI_{AV}, followed by the chlorido derivative **d1**, both surpassing cisplatin (Table 2). The descending order of SI_{AV} for ZL-34 was **d3** > **d1** > **2** > **3** > **d2** = cisplatin. On the other hand, **d3** showed relatively moderate cytotoxicity (IC_{50} after 72 hours ≈ 505 μM), especially if compared to complex **2** (IC_{50} ≈ 183 μM at 72 hours) and **d2** (IC_{50} ≈ 189 μM at 72 hours). Therefore **2** and **d2** appear the most promising compounds for tumor types related to ZL-34 cells as the only nucleoside-bound platinum agents among those tested to exhibit a significant cytotoxicity and a selectivity similar or slightly higher than that of cisplatin. This suggests the need for further studies on complexes **2** and **d2** to maximize both selectivity and potency when targeting the ZL-34 and other related tumor types, for which cisplatin remains more immediately cytotoxic but less selective overall.

Considering together, these comparative results (Table 2) indicate substantial potential for the here reported platinated nucleoside derivatives in designing possible innovative therapeutic strategies. By selecting halido ligands (Cl, Br, I) and nucleobase moieties (Guo or dGuo), one could fine-tune both cytotoxic potency and tumor selectivity, guiding future development and further preclinical evaluation of these promising anticancer agents.

Experimental section

Reagents and methods

All commercially available reagents and solvents were obtained from Sigma-Aldrich and used as received, without further purification. All reactions were performed under ambient conditions. NMR spectra were acquired using a Bruker Avance III 400 NMR spectrometer, equipped with inverse detection probes and *z*-gradient capabilities for gradient-enhanced NMR spectroscopy. Two-dimensional [^{1}H,^{195}Pt]-HETCOR and ^{1}H NMR spectra were acquired using H_2O/D_2O (90 : 10) as the solvent. The ^{1}H NMR spectra were calibrated against tetramethylsilane (TMS), using the residual proton signal from H_2O/D_2O (90 : 10) ($\delta(^{1}H)$ = 4.7 ppm) as the internal reference. ^{195}Pt NMR chemical shifts were referenced to $H_2[PtCl_6]$ [$\delta(^{195}Pt)$ = 0 ppm] in H_2O/D_2O (90 : 10) as the external reference. The use of H_2O/D_2O (90 : 10) as the solvent ensures the detection of exchangeable protons (*e.g.*, $-NH_3$ and $-NH_2$ groups). In pure D_2O, these labile protons would rapidly undergo deuterium exchange, effectively replacing protons with deuterons and making them undetectable in the ^{1}H NMR spectrum. By maintaining a 90% H_2O environment, the solvent acts as a reservoir for protons, preserving the protonation state of exchangeable groups and enabling their observation. Additionally, a small fraction of D_2O (10%) provides a sufficient deuterium signal for the NMR spectrometer's "lock system", which stabilizes the magnetic field during data acquisition. Coupling constants (*J* values) are given in Hertz, and the NMR signal multiplicities are noted as follows: s (singlet), d (doublet), dd (doublet of doublets), t (triplet), m (multiplet), and b (broad). Mass spectrometry (MS) analysis was conducted by dissolving complexes (**1–3**, **d1–d3**) in water, with sample injections handled *via* a Chemyx Inc. Model Fusion 101 syringe pump. Electrospray ionization (ESI) and high-resolution mass spectrometry (HRMS) spectra were collected using a Thermo Fisher Scientific Q-Exactive HPLC-FT/MS system under standard conditions: positive ion mode, flow rate of 0.200 mL min^{-1}, sheath gas at 5.0 L min^{-1}, capillary temperature at 320 °C, spray voltage at 4500 V, and a mass range of 3 000 000–8 000 000 *m*/*z*. Platinum concentration was measured by Inductively Coupled Plasma – Atomic Emission Spectroscopy (ICP-AES) using a Thermo iCAP 6000 spectrometer. To quantify platinum levels, the samples were subjected to acid digestion using 10 mL of ultrapure nitric acid (2%) for 24 hours at room temperature. Before analysis, the samples were filtered to remove any particulate matter that could potentially interfere with the spectrometer. Calibration was carried out using a four-point standard curve (1, 10, 100, and 1000 μg L^{-1}) to ensure analytical precision.[64]

Synthesis of platinum complexes

Platinum complexes *cis*-[Pt(NH$_3$)$_2$(*N7*-Guo/dGuo)Cl] (**1** and **d1**) and *cis*-[Pt(NH$_3$)$_2$(*N7*-Guo/dGuo)Br] (**2** and **d2**) were synthesized following a previously reported method[10,36,54] with minor modifications. Briefly, *cis*-[Pt(NH$_3$)$_2$Cl$_2$] (for complexes **1** and **d1**) (100 mg, 0.332 mmol) or *cis*-[Pt(NH$_3$)$_2$Br$_2$] (for complexes **2** and **d2**) (100 mg, 0.257 mmol) and an equimolar amount of $AgNO_3$ were dissolved in 5 mL of *N*,*N*-dimethylformamide (DMF) and stirred at room temperature for 24 hours. The resulting AgX (X = Cl or Br) precipitate was then removed by centrifugation. The clear supernatant was further reacted with an equimolar amount of guanosine (for complexes **1** and **2**) or 2′-deoxyguanosine monohydrate (for complexes **d1** and **d2**) and stirred for an additional 24 hours. Upon completion of the reaction, the DMF solvent was evaporated under reduced pressure, leaving a solid residue. This residue was washed three times with dichloromethane (CH_2Cl_2), with stirring each time, and then dried. Finally, the crude product was purified by recrystallization from hot water, repeating the process three times, and then dried in air.

***cis*-[Pt(NH$_3$)$_2$(*N7*-Guo)Cl]NO$_3$ (1).** Yield: 110 mg, 54%. Anal. calcd (found) for $C_{10}H_{19}ClN_8O_8Pt$: Pt, 31.99 (31.71). MS (ESI) *m*/*z* calculated for $C_{10}H_{19}ClN_7O_5Pt$ $[M]^+$: 547.0784, found: $[M + H]^+$ 548.0776. ^{1}H NMR (400 MHz, H_2O/D_2O 90 : 10, 300 K) δ: 8.41 (s, 1H, H-8), 6.48 (s, 2H, NH_2), 5.90 (d, 1H, H-1′, *J* = 4.82 Hz), 4.34 (t, 1H, H-3′, *J* = 4.96 Hz), 4.24 (s, 3H, NH_3), 4.17 (q, 1H, H-4′, *J* = 3.35 Hz), 4.06 (s, 3H, NH_3), 3.88–3.75 (m, 2H, H-5′ & H-5″), $\delta(^{195}Pt)$ −2282 ppm.

***cis*-[Pt(NH$_3$)$_2$(*N7*-Guo)Br]NO$_3$ (2).** Yield: 81 mg, 48%. Anal. calcd (found) for $C_{10}H_{19}BrN_8O_8Pt$: Pt, 29.78 (29.90). MS (ESI) *m*/*z* calculated for $C_{10}H_{19}BrN_7O_5Pt$ $[M]^+$: 591.0279, found: $[M + H]^+$ 592.0282. ^{1}H NMR (400 MHz, H_2O/D_2O 90 : 10, 300 K) δ: 8.44 (s, 1H, H-8), 6.47 (s, 2H, NH_2), 5.89 (d, 1H, H-1′, *J* = 4.70 Hz), 4.33 (t, 1H, H-3′, *J* = 4.99 Hz), 4.23 (s, 3H, NH_3), 4.16 (q, 1H, H-4′, *J* = 3.81 Hz), 4.04 (s, 3H, NH_3), 3.88–3.75 (m, 2H, H-5′ & H-5″), $\delta(^{195}Pt)$ −2414 ppm.

***cis*-[Pt(NH$_3$)$_2$(*N7*-dGuo)Cl]NO$_3$·H$_2$O (d1).** Yield: 85.5 mg, 42%. Anal. calcd (found) for $C_{10}H_{21}ClN_8O_8Pt$: Pt, 31.88 (31.18). MS (ESI) *m*/*z* calculated for $C_{10}H_{19}ClN_7O_4Pt$ $[M]^+$: 531.0835, found: $[M + H]^+$ 532.0840. ^{1}H NMR (400 MHz, H_2O/D_2O 90 : 10, 300 K) δ: 8.36 (s, 1H, H-8), 6.45 (s, 2H, NH_2), 6.27 (t, 1H, H-1′, *J* = 6.50 Hz), 4.23 (s, 3H, NH_3), 4.07 (q, 1H, H-4′, *J* = 4.08 Hz), 4.06 (s, 3H, NH_3), 3.79–3.69 (m, 2H, H-5′ & H-5″), 2.69 (m, 1H, H-2′), 2.49 (m, 1H, H-2″), $\delta(^{195}Pt)$ −2282 ppm.

***cis*-[Pt(NH$_3$)$_2$(*N7*-dGuo)Br]NO$_3$·H$_2$O (d2).** Yield: 59.2 mg, 35%. Anal. calcd (found) for $C_{10}H_{21}BrN_8O_8Pt$: Pt, 29.72 (29.17). MS (ESI) *m*/*z* calculated for $C_{10}H_{19}BrN_7O_4Pt$ $[M]^+$: 575.0330, found: $[M + H]^+$ 576.0326. ^{1}H NMR (400 MHz, H_2O/D_2O 90 : 10, 300 K) δ: 8.39 (s, 1H, H-8), 6.44 (s, 2H, NH_2), 6.26 (t, 1H, H-1′, *J* = 6.48 Hz), 4.22 (s, 3H, NH_3), 4.07 (q, 1H, H-4′, *J* = 4.08 Hz), 4.04 (s, 3H, NH_3), 3.79–3.68 (m, 2H, H-5′ & H-5″), 2.69 (m, 1H, H-2′), 2.49 (m, 1H, H-2″), $\delta(^{195}Pt)$ −2413 ppm.

Synthesis of the platinum complexes 3 and d3

The aqueous solution of chlorido precursors (**1** or **d1**) was reacted with an equimolar aqueous solution of $AgNO_3$. After the AgCl was removed, one equivalent of KI was added, initiating an immediate reaction. The solvent was then removed under reduced pressure. The resulting solid was washed thoroughly with cold water three times and dried to yield the pure iodido complexes *cis*-[$Pt(NH_3)_2$(*N7*-Guo/dGuo)I]NO_3 (**3** and **d3**).

***cis*-[$Pt(NH_3)_2$(*N7*-Guo)I]NO_3 (3).** Yield: 66.7 mg, 58%. Anal. calcd (found) for $C_{10}H_{19}IN_8O_8Pt$: Pt, 27.82 (27.90). MS (ESI) *m*/*z* calculated for $C_{10}H_{19}IN_7O_5Pt$ $[M]^+$: 639.0140, found: $[M]^+$ 639.0171. ^{1}H NMR (400 MHz, H_2O/D_2O 90 : 10, 300 K) δ: 8.46 (s, 1H, H-8), 6.45 (s, 2H, NH_2), 5.84 (d, 1H, H-1′, J = 4.66 Hz), 4.29 (t, 1H, H-3′, J = 4.96 Hz), 4.18 (s, 3H, NH_3), 4.13 (q, 1H, H-4′, J = 3.92 Hz), 3.99 (s, 3H, NH_3), 3.84–3.71 (m, 2H, H-5′ & H-5″), δ(^{195}Pt) −2730 ppm.

***cis*-[$Pt(NH_3)_2$(*N7*-dGuo)I]$NO_3 \cdot H_2O$ (d3).** Yield: 50.6 mg, 44%. Anal. calcd (found) for $C_{10}H_{21}IN_8O_8Pt$: Pt, 27.74 (27.31). MS (ESI) *m*/*z* calculated for $C_{10}H_{19}IN_7O_4Pt$ $[M]^+$: 623.0191, found: $[M]^+$ 623.0216. ^{1}H NMR (400 MHz, H_2O/D_2O 90 : 10, 300 K) δ: 8.41 (s, 1H, H-8), 6.43 (s, 2H, NH_2), 6.21 (t, 1H, H-1′, J = 6.43 Hz), 4.18 (s, 3H, NH_3), 4.02 (q, 1H, H-4′, J = 4.12 Hz), 3.98 (s, 3H, NH_3), 3.74–3.64 (m, 2H, H-5′ & H-5″), 2.65 (m, 1H, H-2′), 2.44 (m, 1H, H-2″), δ(^{195}Pt) −2729 ppm.

Cell cultures

The following cell lines derived from frozen stocks MCF-7 (human breast adenocarcinoma): HTB-22™, HeLa (human cervical adenocarcinoma): CRM-CCL-2™, Caki-1 (human renal carcinoma): HTB-46™, HK-2 (human kidney proximal tubule epithelial cells): CRL-2190™, Raji (human Burkitt's lymphoma): CCL-86™ were purchased from the American Type Cell Culture collection (ATCC), Manassas, VA, USA. ZL-34 (human pleural mesothelioma) cell line (cat. no. 11120713) was purchased from Sigma-Aldrich, St Louis, MO, USA.

ZL-34, Raji and MCF-7 cells were cultured in RPMI 1640 medium (EuroClone, Pero, MI) supplemented with 10% (v/v) heat-inactivated fetal bovine serum (FBS), 2 mM L-glutamine, penicillin (100 U mL^{-1}), and streptomycin (100 μg mL^{-1}). HeLa, Caki-1, and HK-2 cells were cultured in Dulbecco's Modified Eagle's medium (DMEM) with 4.5 g L^{-1} glucose (EuroClone, Pero, MI), supplemented with 10% (v/v) heat-inactivated FBS, 2 mM L-glutamine, penicillin (100 U mL^{-1}), and streptomycin (100 μg mL^{-1}). Cells were grown in a humidified incubator with 5% CO_2 in air at 37 °C and were used for biological assays upon reaching 70–80% confluence. Cells were sub-cultured for further study after reaching 80% confluence.

Cell viability assays

SRB assay. The viability of Caki-1, HeLa, MCF-7, ZL-34, and HK-2 cell lines was assessed using the sulforhodamine B (SRB) colorimetric assay.[65,66] Approximately 100 μl of cell suspension was added to each well of a 96-well microtiter plate (90 000 cells per ml). For cell treatments, the Pt-compounds were dissolved in Dulbecco's phosphate-buffered saline (PBS) to prepare a stock solution (1 mM), from which subsequent dilutions ranging from 1 to 1000 μM were prepared. After overnight incubation, the cells were treated with various concentrations (0, 1, 10, 50, 100, 200, 500, and 1000 μM) of cisplatin and platinum(II) nucleoside complexes for 24, 48 and 72 h. At the end of each treatment period, 100 μL of ice-cold 10% (w/v) trichloroacetic acid was added to each well and incubated for 30 min at 4 °C. The plates were then washed five times with double-distilled water and allowed to air-dry overnight. Subsequently, 60 μL of 0.4% (w/v) SRB solution was added to each well and incubated for 20 min, followed by four washes with 1% (v/v) acidic acetic acid. Finally, the SRB was solubilized in 200 μL of 10 mM unbuffered Tris-base solution, and the absorbance was measured at 560 nm using a spectrophotometer.[67] The percentage of cell survival was calculated as the ratio of the absorbance of treated cells to that of vehicle-treated control cells.

MTT assays. The viability of non-adherent Raji cells was assessed using the MTT assay, which is more suitable than the SRB assay for suspension cells. Since Raji cells do not adhere to the plate, they are prone to being lost during the washing steps. The MTT assay avoids this issue because its formazan product remains inside the cells until dissolved, ensuring a more reliable viability measurement. Cells were treated with Pt(II) compounds as previously described. After treatment, the medium was removed, and 10 μL of MTT solution was added to each well containing Raji cells. Following a 3-hour incubation, 100 μL of isopropanol was added to dissolve the purple formazan crystals.[68] An additional 100 μL of HCl-isopropanol was then added directly to the wells after platinum compounds exposure. Absorbance was measured at 595 nm using a spectrophotometer. Cell viability (%) was calculated as the absorbance percentage relative to untreated control cells.

Conclusions

In this study, we synthesized and characterized six Pt(II) complexes of the form *cis*-[$Pt(NH_3)_2$(*N7*-Guo)X]$^+$ (X = Cl, **1**; Br, **2**; I, **3**) and *cis*-[$Pt(NH_3)_2$(*N7*-dGuo)X]$^+$ (X = Cl, **d1**; Br, **d2**; I, **d3**). We also assessed their effects in multiple cancer cell lines (HeLa, MCF-7, Raji, Caki-1, ZL-34) as well as a proximal tubule epithelial cell line (HK-2). The impact of different coordinated halido ligands on cytotoxicity of the examined six monofunctional platinated nucleosides resulted significant. Our finding confirmed various recent investigations on metal complexes showing how the halido ligand modulates both the reactivity and stability of these metal-drugs, thereby altering their cytotoxic profiles against diverse cancer cell lines.[49,69,70]

In the HeLa cells, the bromido-complex **d2** displayed the highest cytotoxicity and selectivity among the tested nucleobase derivatives, followed closely by complex **2**, which was slightly less potent yet still more selective than cisplatin (Tables 1 and 2). A similar pattern emerged in MCF-7 breast

cancer cells but shifted toward the iodido species, where **d3** outperformed the other nucleobase derivatives in both cytotoxicity and selectivity. Complex **3** was moderately effective in these cells but remained less selective than **d3**, although both complexes surpassed cisplatin in terms of selectivity.

In Raji cells, complex **2** emerged as the most cytotoxic agent among the nucleobase derivatives, followed by **d2**. Notably, **1**, **d1** and **2**, **d2** all demonstrated superior selectivity relative to cisplatin, suggesting further potential in the lymphoma treatment. In Caki-1 cells, **d2** was the most cytotoxic among the nucleobase derivatives; however, complexes **1** and **d1** exhibited the highest selectivity, again surpassing cisplatin (Table 2).

With ZL-34, the iodido derivative **d3** presented the greatest selectivity but only moderate cytotoxicity, while complex **2** and **d2** achieved stronger cytotoxic effects (albeit with slightly reduced selectivity), remaining more selective than cisplatin overall.

Although these newly synthesized complexes generally showed lower absolute cytotoxicity than cisplatin, their structural features, particularly the identity of the halido ligand (Cl, Br, or I), strongly influence their biological activity and selectivity profiles. Bromido-substituted species (**2**, **d2**) often exhibited elevated potency, underscoring the prospect of nucleoside-based platinum agents in the treatment of lymphoid and myeloid malignancies.[27,71] Likewise, iodido complexes (**3**, **d3**) demonstrate marked cytotoxicity and selectivity in MCF-7 cells, illustrating that the type of halido ligand can tailor activity in a tumor-selective manner.

Importantly, all six Pt(II) nucleoside complexes displayed significantly reduced cytotoxicity in the healthy immortalized cell line (HK-2), frequently showing IC_{50} values beyond the maximum tested concentration. While they were not as potent as cisplatin in most investigated tumor models, their higher Selectivity Indexes suggest possible available therapeutic windows in which cancer cells are more strongly affected than healthy cells. Overall, the halido substituent emerges as a crucial factor in tuning both cytotoxic properties and overall selectivity, offering a strategic route to develop Pt(II)-based agents with improved therapeutic and fewer off-target effects. According to the here reported results for Guo and dGuo platinated derivatives, this is particularly true in the following tumor cell lines, showing the better compromise between cytotoxicity and selectivity for each of the selected tumors: HeLa (**2**, **d2**); MCF-7 (**3**, **d3**); Raji (**2**); Caki-1 (**1**, **d2**); ZL-34 (**2**, **d2**).

Author contributions

Asjad Ali: conceptualization, software, data curation, formal analysis, investigation, and writing–original draft. Gianluca Rovito: software, data curation, formal analysis, investigation, and writing–original draft. Erika Stefàno: data curation, formal analysis, investigation, and writing–original draft. Federica De Castro: validation, visualization, and writing–review and editing. Giuseppe Ciccarella: data curation, investigation and visualization. Danilo Migoni: formal analysis. Elisa Panzarini: validation and visualization. Antonella Muscella: validation and visualization. Santo Marsigliante: supervision, validation, and visualization. Michele Benedetti: supervision, validation, visualization, and writing–review and editing. Francesco Paolo Fanizzi: visualization, and writing–review and editing.

Data availability

The data that support the findings of this study are available from the corresponding author upon reasonable request.

Conflicts of interest

There are no conflicts to declare.

References

1 R. L. Siegel, A. N. Giaquinto and A. Jemal, Cancer statistics, 2024, *CA-Cancer J. Clin.*, 2024, **74**, 12–49.
2 E. J. Anthony, E. M. Bolitho, H. E. Bridgewater, O. W. L. Carter, J. M. Donnelly, C. Imberti, E. C. Lant, F. Lermyte, R. J. Needham, M. Palau, P. J. Sadler, H. Shi, F.-X. Wang, W.-Y. Zhang and Z. Zhang, Metallodrugs are unique: opportunities and challenges of discovery and development, *Chem. Sci.*, 2020, **11**, 12888–12917.
3 T. C. Johnstone, G. Y. Park and S. J. Lippard, Understanding and improving platinum anticancer drugs–phenanthriplatin, *Anticancer Res.*, 2014, **34**, 471–476.
4 T. C. Johnstone, K. Suntharalingam and S. J. Lippard, The Next Generation of Platinum Drugs: Targeted Pt(II) Agents, Nanoparticle Delivery, and Pt(IV) Prodrugs, *Chem. Rev.*, 2016, **116**, 3436–3486.
5 I. A. Riddell, T. C. Johnstone, G. Y. Park and S. J. Lippard, Nucleotide Binding Preference of the Monofunctional Platinum Anticancer-Agent Phenanthriplatin, *Chem. – Eur. J.*, 2016, **22**, 7574–7581.
6 J. Zhou, Y. Kang, L. Chen, H. Wang, J. Liu, S. Zeng and L. Yu, The Drug-Resistance Mechanisms of Five Platinum-Based Antitumor Agents, *Front. Pharmacol.*, 2020, **11**, 343.
7 A. M. P. Romani, Cisplatin in cancer treatment, *Biochem. Pharmacol.*, 2022, **206**, 115323.
8 G.-B. Liang, Y.-C. Yu, J.-H. Wei, W.-B. Kuang, Z.-F. Chen and Y. Zhang, Design, synthesis and biological evaluation of naphthalenebenzimidizole platinum(II) complexes as potential antitumor agents, *Eur. J. Med. Chem.*, 2020, **188**, 112033.
9 A. Ali, E. Stefàno, F. De Castro, G. Ciccarella, G. Rovito, S. Marsigliante, A. Muscella, M. Benedetti and F. P. Fanizzi, Synthesis, Characterization, and Cytotoxicity Evaluation of Novel Water-Soluble Cationic Platinum(II) Organometallic Complexes with Phenanthroline and Imidazolic Ligands, *Chem. – Eur. J.*, 2024, **30**, e202401064.

10 L. S. Hollis, W. I. Sundquist, J. N. Burstyn, W. J. Heiger-Bernays, S. F. Bellon, K. J. Ahmed, A. R. Amundsen, E. W. Stern and S. J. Lippard, Mechanistic Studies of a Novel Class of Trisubstituted Platinum(II) Antitumor Agents, *Cancer Res.*, 1991, **51**, 1866–1875.
11 A. A. Almaqwashi, W. Zhou, M. N. Naufer, I. A. Riddell, Ö. H. Yilmaz, S. J. Lippard and M. C. Williams, DNA Intercalation Facilitates Efficient DNA-Targeted Covalent Binding of Phenanthriplatin, *J. Am. Chem. Soc.*, 2019, **141**, 1537–1545.
12 J.-P. Macquet and J.-L. Butour, Platinum-Amine Compounds: Importance of the Labile and Inert Ligands for Their Pharmacological Activities Toward L1210 Leukemia Cells, *JNCI, J. Natl. Cancer Inst.*, 1983, **70**, 899–905.
13 S. Dilruba and G. V. Kalayda, Platinum-based drugs: past, present and future, *Cancer Chemother. Pharmacol.*, 2016, **77**, 1103–1124.
14 M. J. Cleare and J. D. Hoeschele, Studies on the antitumor activity of group VIII transition metal complexes. Part I. Platinum(II) complexes, *Bioinorg. Chem.*, 1973, **2**, 187–210.
15 M. J. Cleare and J. D. Hoeschele, Anti-tumour Platinum Compounds, *Platinum Met. Rev.*, 1973, **17**, 2–13.
16 W. I. Sundquist, D. P. Bancroft and S. J. Lippard, Synthesis, characterization, and biological activity of *cis*-diammineplatinum(II) complexes of the DNA intercalators 9-aminoacridine and chloroquine, *J. Am. Chem. Soc.*, 1990, **112**, 1590–1596.
17 S. Jin, Y. Guo, Z. Guo and X. Wang, Monofunctional platinum(II) anticancer agents, *Pharmaceuticals*, 2021, **14**, 133.
18 G. Y. Park, J. J. Wilson, Y. Song and S. J. Lippard, Phenanthriplatin, a monofunctional DNA-binding platinum anticancer drug candidate with unusual potency and cellular activity profile, *Proc. Natl. Acad. Sci. U. S. A.*, 2012, **109**, 11987–11992.
19 M. W. Kellinger, G. Y. Park, J. Chong, S. J. Lippard and D. Wang, Effect of a Monofunctional Phenanthriplatin-DNA Adduct on RNA Polymerase II Transcriptional Fidelity and Translesion Synthesis, *J. Am. Chem. Soc.*, 2013, **135**, 13054–13061.
20 T. C. Johnstone and S. J. Lippard, The Chiral Potential of Phenanthriplatin and Its Influence on Guanine Binding, *J. Am. Chem. Soc.*, 2014, **136**, 2126–2134.
21 D. Veclani, A. Melchior, M. Tolazzi and J. P. Cerón-Carrasco, Using Theory To Reinterpret the Kinetics of Monofunctional Platinum Anticancer Drugs: Stacking Matters, *J. Am. Chem. Soc.*, 2018, **140**, 14024–14027.
22 S. Zhang, K. S. Lovejoy, J. E. Shima, L. L. Lagpacan, Y. Shu, A. Lapuk, Y. Chen, T. Komori, J. W. Gray, X. Chen, S. J. Lippard and K. M. Giacomini, Organic Cation Transporters Are Determinants of Oxaliplatin Cytotoxicity, *Cancer Res.*, 2006, **66**, 8847–8857.
23 K. S. Lovejoy, R. C. Todd, S. Zhang, M. S. McCormick, J. A. D'Aquino, J. T. Reardon, A. Sancar, K. M. Giacomini and S. J. Lippard, *cis*-Diammine(pyridine)chloroplatinum (II), a monofunctional platinum(II) antitumor agent: Uptake, structure, function, and prospects, *Proc. Natl. Acad. Sci. U. S. A.*, 2008, **105**, 8902–8907.
24 S. Soodvilai, P. Meetam, L. Siangjong, R. Chokchaisiri, A. Suksamrarn and S. Soodvilai, Germacrone Reduces Cisplatin-Induced Toxicity of Renal Proximal Tubular Cells *via* Inhibition of Organic Cation Transporter, *Biol. Pharm. Bull.*, 2020, **43**, 1693–1698.
25 D. Wang, G. Zhu, X. Huang and S. J. Lippard, X-ray structure and mechanism of RNA polymerase II stalled at an antineoplastic monofunctional platinum-DNA adduct, *Proc. Natl. Acad. Sci. U. S. A.*, 2010, **107**, 9584–9589.
26 C. M. Galmarini, J. R. Mackey and C. Dumontet, Nucleoside analogues and nucleobases in cancer treatment, *Lancet Oncol.*, 2002, **3**, 415–424.
27 F. De Castro, E. Stefàno, E. De Luca, M. Benedetti and F. P. Fanizzi, Platinum-Nucleos(t)ide Compounds as Possible Antimetabolites for Antitumor/Antiviral Therapy: Properties and Perspectives, *Pharmaceutics*, 2023, **15**, 941.
28 E. De Clercq, New Nucleoside Analogues for the Treatment of Hemorrhagic Fever Virus Infections, *Chem. – Asian J.*, 2019, **14**, 3962–3968.
29 N. Tsesmetzis, C. B. J. Paulin, S. G. Rudd and N. Herold, Nucleobase and Nucleoside Analogues: Resistance and Re-Sensitisation at the Level of Pharmacokinetics, Pharmacodynamics and Metabolism, *Cancers*, 2018, **10**, 240.
30 L. P. Jordheim, D. Durantel, F. Zoulim and C. Dumontet, Advances in the development of nucleoside and nucleotide analogues for cancer and viral diseases, *Nat. Rev. Drug Discovery*, 2013, **12**, 447–464.
31 P. B. Matthew, M. B. Kayla and A. L. Vladislav, Base-Modified Nucleosides as Chemotherapeutic Agents: Past and Future, *Curr. Top. Med. Chem.*, 2016, **16**, 1231–1241.
32 A. Abdullah Al Awadh, Nucleotide and nucleoside-based drugs: past, present, and future, *Saudi J. Biol. Sci.*, 2022, **29**, 103481.
33 P. Lunetti, A. Romano, C. Carrisi, D. Antonucci, T. Verri, G. E. De Benedetto, V. Dolce, F. P. Fanizzi, M. Benedetti and L. Capobianco, Platinated Nucleotides are Substrates for the Human Mitochondrial Deoxynucleotide Carrier (DNC) and DNA Polymerase γ: Relevance for the Development of New Platinum-Based Drugs, *ChemistrySelect*, 2016, **1**, 4633–4637.
34 Q. Yang, Y. H. Nie, M. B. Cai, Z. M. Li, H. B. Zhu and Y. R. Tan, Gemcitabine Combined with Cisplatin Has a Better Effect in the Treatment of Recurrent/Metastatic Advanced Nasopharyngeal Carcinoma, *Drug Des., Dev. Ther.*, 2023, **16**, 1191–1198.
35 A. M. Mosconi, L. Crinò and M. Tonato, Combination therapy with gemcitabine in non-small cell lung cancer, *Eur. J. Cancer*, 1997, **33**, S14–S17.
36 L. S. Hollis, A. R. Amundsen and E. W. Stern, Chemical and biological properties of a new series of *cis*-diammineplatinum(II) antitumor agents containing three nitrogen donors: *cis*-$[Pt(NH_3)_2(N\text{-donor})Cl]^+$, *J. Med. Chem.*, 1989, **32**, 128–136.

37 F. De Castro, E. De Luca, M. Benedetti and F. P. Fanizzi, Platinum compounds as potential antiviral agents, *Coord. Chem. Rev.*, 2022, **451**, 214276.
38 K. K. Nayak, R. Bhattacharyya and P. Maity, Synthesis, characterization, and in vitro cytotoxic effects of $K_4[PtCl_2ATP]$, *J. Inorg. Biochem.*, 1991, **41**, 293–298.
39 S. Kirschner, Y.-K. Wei, D. Francis and J. G. Bergman, Anticancer and potential antiviral activity of complex inorganic compounds, *J. Med. Chem.*, 1966, **9**, 369–372.
40 M. S. Ali, S. R. Ali Khan, H. Ojima, I. Y. Guzman, K. H. Whitmire, Z. H. Siddik and A. R. Khokhar, Model platinum nucleobase and nucleoside complexes and antitumor activity: X-ray crystal structure of $[Pt^{IV}$(*trans*-1R,2R-diaminocyclohexane)*trans*-(acetate)$_2$(9-ethylguanine)Cl$]NO_3 \cdot H_2O$, *J. Inorg. Biochem.*, 2005, **99**, 795–804.
41 R. D. Kuchta, Nucleotide Analogues as Probes for DNA and RNA Polymerases, *Curr. Protoc. Chem. Biol.*, 2010, **2**, 111–124.
42 D. A. Sartori, B. Miller, U. Bierbach and N. Farrell, Modulation of the chemical and biological properties of trans platinum complexes: monofunctional platinum complexes containing one nucleobase as potential antiviral chemotypes, *JBIC, J. Biol. Inorg. Chem.*, 2000, **5**, 575–583.
43 N. Margiotta, A. Bergamo, G. Sava, G. Padovano, E. de Clercq and G. Natile, Antiviral properties and cytotoxic activity of platinum(II) complexes with 1,10-phenanthrolines and acyclovir or penciclovir, *J. Inorg. Biochem.*, 2004, **98**, 1385–1390.
44 F. De Castro, E. De Luca, C. R. Girelli, A. Barca, A. Romano, D. Migoni, T. Verri, M. Benedetti and F. P. Fanizzi, First evidence for N7-Platinated Guanosine derivatives cell uptake mediated by plasma membrane transport processes, *J. Inorg. Biochem.*, 2022, **226**, 111660.
45 C. Carrisi, D. Antonucci, P. Lunetti, D. Migoni, C. R. Girelli, V. Dolce, F. P. Fanizzi, M. Benedetti and L. Capobianco, Transport of platinum bonded nucleotides into proteoliposomes, mediated by Drosophila melanogaster thiamine pyrophosphate carrier protein (DmTpc1), *J. Inorg. Biochem.*, 2014, **130**, 28–31.
46 M. Benedetti, C. Ducani, D. Migoni, D. Antonucci, V. M. Vecchio, A. Ciccarese, A. Romano, T. Verri, G. Ciccarella and F. P. Fanizzi, Experimental evidence that a DNA polymerase can incorporate N7-platinated guanines to give platinated DNA, *Angew. Chem., Int. Ed. Engl.*, 2008, **47**, 507.
47 B. Lippert and P. J. Sanz Miguel, Beyond sole models for the first steps of Pt-DNA interactions: Fundamental properties of mono(nucleobase) adducts of Pt^{II} coordination compounds, *Coord. Chem. Rev.*, 2022, **465**, 214566.
48 Y. Lu, Y. Liu, Z. Xu, H. Li, H. Liu and W. Zhu, Halogen bonding for rational drug design and new drug discovery, *Expert Opin. Drug Discovery*, 2012, **7**, 375–383.
49 A. Sarkar, S. Acharya, K. Khushvant, K. Purkait and A. Mukherjee, Cytotoxic Ru^{II}-*p*-cymene complexes of an anthraimidazoledione: halide dependent solution stability, reactivity and resistance to hypoxia deactivation, *Dalton Trans.*, 2019, **48**, 7187–7197.
50 S. K. Goetzfried, P. Kapitza, C. M. Gallati, A. Nindl, M. Cziferszky, M. Hermann, K. Wurst, B. Kircher and R. Gust, Investigations of the reactivity, stability and biological activity of halido (NHC)gold(I) complexes, *Dalton Trans.*, 2022, **51**, 1395–1406.
51 J. J. Wilson and S. J. Lippard, Synthetic Methods for the Preparation of Platinum Anticancer Complexes, *Chem. Rev.*, 2014, **114**, 4470–4495.
52 M. Fanelli, M. Formica, V. Fusi, L. Giorgi, M. Micheloni and P. Paoli, New trends in platinum and palladium complexes as antineoplastic agents, *Coord. Chem. Rev.*, 2016, **310**, 41–79.
53 C. Mügge, T. Marzo, L. Massai, J. Hildebrandt, G. Ferraro, P. Rivera-Fuentes, N. Metzler-Nolte, A. Merlino, L. Messori and W. Weigand, Platinum(II) Complexes with O,S Bidentate Ligands: Biophysical Characterization, Antiproliferative Activity, and Crystallographic Evidence of Protein Binding, *Inorg. Chem.*, 2015, **54**, 8560–8570.
54 B. Lippert, R. Pfab and D. Neugebauer, The role of N(1) coordianted thynine in 'platinum thymine blue', *Inorg. Chim. Acta*, 1979, **37**, L495–L497.
55 V. X. Jin, S. I. Tan and J. D. Ranford, Platinum(II) triammine antitumour complexes: structure–activity relationship with guanosine 5′-monophosphate (5′-GMP), *Inorg. Chim. Acta*, 2005, **358**, 677–686.
56 M. Masuda, T. Suzuki, M. D. Friesen, J.-L. Ravanat, J. Cadet, B. Pignatelli, H. Nishino and H. Ohshima, Chlorination of Guanosine and Other Nucleosides by Hypochlorous Acid and Myeloperoxidase of Activated Human Neutrophils: Catalysis by Nicotine and Trimethylamine, *J. Biol. Chem.*, 2001, **276**, 40486–40496.
57 M. Benedetti, F. De Castro, P. Papadia, D. Antonucci and F. P. Fanizzi, ^{195}Pt and ^{15}N NMR Data in Square Planar Platinum(II) Complexes of the Type $[Pt(NH_3)X]$ (X = Combination of Halides): "NMR Effective Molecular Radius" of Coordinated Ammonia, *Eur. J. Inorg. Chem.*, 2020, **2020**, 3395–3401.
58 M. Benedetti, F. de Castro, D. Antonucci, P. Papadia and F. P. Fanizzi, General cooperative effects of single atom ligands on a metal: a ^{195}Pt NMR chemical shift as a function of coordinated halido ligands' ionic radii overall sum, *Dalton Trans.*, 2015, **44**, 15377–15381.
59 M. Benedetti, F. De Castro and F. P. Fanizzi, Square-Planar Pt^{II} versus Octahedral Pt^{IV} Halido Complexes: ^{195}Pt NMR Explained by a Simple Empirical Approach, *Eur. J. Inorg. Chem.*, 2016, **2016**, 3957–3962.
60 T. G. Appleton, J. R. Hall and S. F. Ralph, Nitrogen-15 and platinum-195 NMR spectra of platinum ammine complexes: *trans*- and *cis*-influence series based on platinum-195-nitrogen-15 coupling constants and nitrogen-15 chemical shifts, *Inorg. Chem.*, 1985, **24**, 4685–4693.
61 L. Patiny and A. Borel, ChemCalc: A Building Block for Tomorrow's Chemical Infrastructure, *J. Chem. Inf. Model.*, 2013, **53**, 1223–1228.

62 S. Scoditti, V. Vigna, E. Dabbish and E. Sicilia, Iodido equatorial ligands influence on the mechanism of action of Pt (IV) and Pt(II) anti-cancer complexes: A DFT computational study, *J. Comput. Chem.*, 2021, **42**, 608–619.

63 X. Wu, L. Liu, Q. Wang, H. Wang, X. Zhao, X. Lin, W. Lv, Y. Niu, T. Lu and Q. Mei, Antitumor Activity and Mechanism Study of Riluzole and Its Derivatives, *Iran. J. Pharm. Res.*, 2020, **19**, e124401.

64 F. De Castro, E. Stefàno, D. Migoni, G. N. Iaconisi, A. Muscella, S. Marsigliante, M. Benedetti and F. P. Fanizzi, Synthesis and Evaluation of the Cytotoxic Activity of Water-Soluble Cationic Organometallic Complexes of the Type [Pt(η^1-C_2H_4OMe)(L)(Phen)]$^+$ (L = NH_3, DMSO; Phen = 1,10-Phenanthroline), *Pharmaceutics*, 2021, **13**, 642.

65 P. Skehan, R. Storeng, D. Scudiero, A. Monks, J. McMahon, D. Vistica, J. T. Warren, H. Bokesch, S. Kenney and M. R. Boyd, New Colorimetric Cytotoxicity Assay for Anticancer-Drug Screening, *JNCI, J. Natl. Cancer Inst.*, 1990, **82**, 1107–1112.

66 M. C. Alley, D. A. Scudiero, A. Monks, M. L. Hursey, M. J. Czerwinski, D. L. Fine, B. J. Abbott, J. G. Mayo, R. H. Shoemaker and M. R. Boyd, Feasibility of Drug Screening with Panels of Human Tumor Cell Lines Using a Microculture Tetrazolium Assay, *Cancer Res.*, 1988, **48**, 589–601.

67 E. Stefàno, L. G. Cossa, F. De Castro, E. De Luca, V. Vergaro, G. My, G. Rovito, D. Migoni, A. Muscella, S. Marsigliante, M. Benedetti and F. P. Fanizzi, Evaluation of the Antitumor Effects of Platinum-Based [Pt(η^1-C_2H_4-OR)(DMSO)(phen)]$^+$ (R = Me, Et) Cationic Organometallic Complexes on Chemoresistant Pancreatic Cancer Cell Lines, *Bioinorg. Chem. Appl.*, 2023, **2023**, 5564624.

68 F. De Castro, M. Benedetti, G. Antonaci, L. Del Coco, S. A. De Pascali, A. Muscella, S. Marsigliante and F. P. Fanizzi, Response of Cisplatin Resistant Skov-3 Cells to [Pt(O,O′-Acac)(γ-Acac)(DMS)] Treatment Revealed by a Metabolomic ^{1}H-NMR Study, *Molecules*, 2018, **23**, 2301.

69 L. G. Lavrenova, T. A. Kuz'menko, A. D. Ivanova, A. I. Smolentsev, V. Y. Komarov, A. S. Bogomyakov, L. A. Sheludyakova and E. V. Vorontsova, Synthesis and magnetic and cytotoxic properties of copper(II) halide complexes with 1,2,4-triazolo[1,5-a] benzimidazoles, *New J. Chem.*, 2017, **41**, 4341–4347.

70 O. Sánchez-Guadarrama, H. López-Sandoval, F. Sánchez-Bartéz, I. Gracia-Mora, H. Höpfl and N. Barba-Behrens, Cytotoxic activity, X-ray crystal structures and spectroscopic characterization of cobalt(II), copper(II) and zinc(II) coordination compounds with 2-substituted benzimidazoles, *J. Inorg. Biochem.*, 2009, **103**, 1204–1213.

71 T. Robak, New nucleoside analogs for patients with hematological malignancies, *Expert Opin. Invest. Drugs*, 2011, **20**, 343–359.